Supplementary Information (SI) for Nanoscale.

Supporting Information

Balancing Interfacial Properties and Porosity in Multiscale Porous Carbon Composite Coatings for Advanced Li-S Battery Separators

Thi Ai Ngoc Bui[1], Thao Nguyen[1], Ching-Kuan Yang[2], Jeng-Kuei Chang[3] and Yu-Sheng Su[1,2]*

[1]International College of Semiconductor Technology, National Yang Ming Chiao Tung University, 1001 Daxue Road, Hsinchu 300093, Taiwan

[2]Industry Academia Innovation School, National Yang Ming Chiao Tung University, 1001 Daxue Road, Hsinchu 300093, Taiwan

[3]Department of Materials Science and Engineering, National Yang Ming Chiao Tung University, 1001 Daxue Road, Hsinchu 300093, Taiwan

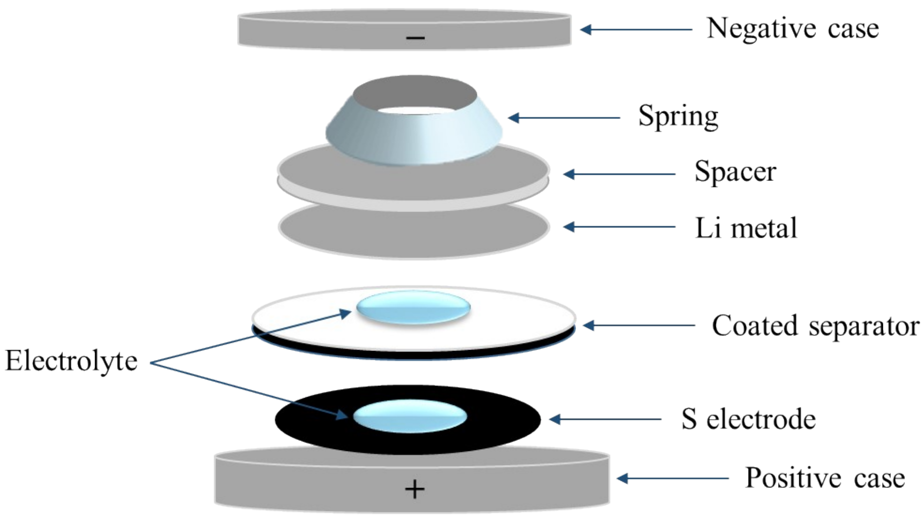

Figure S1. Schematic illustration of the CR2032 coin cell configuration.

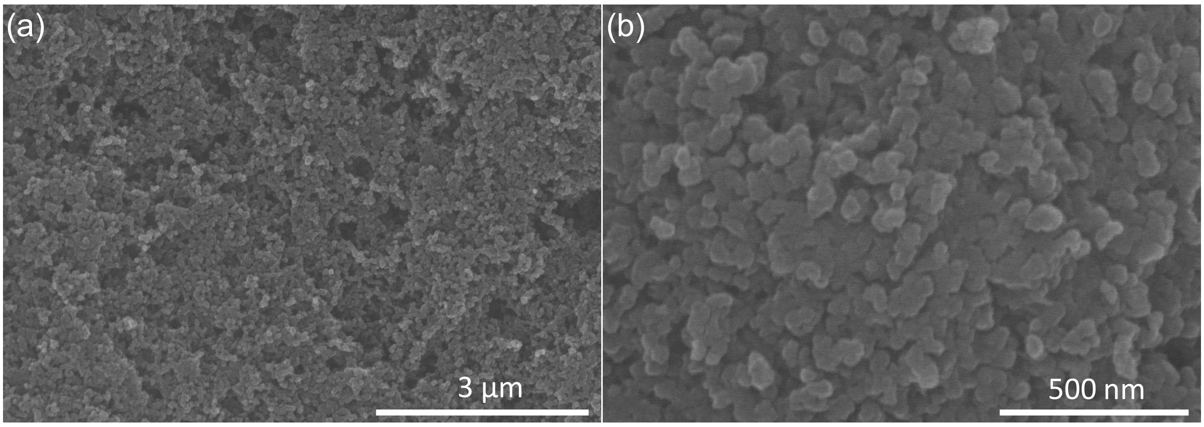

Figure S2. SEM images of MPC material at (a) low and (b) high magnification.

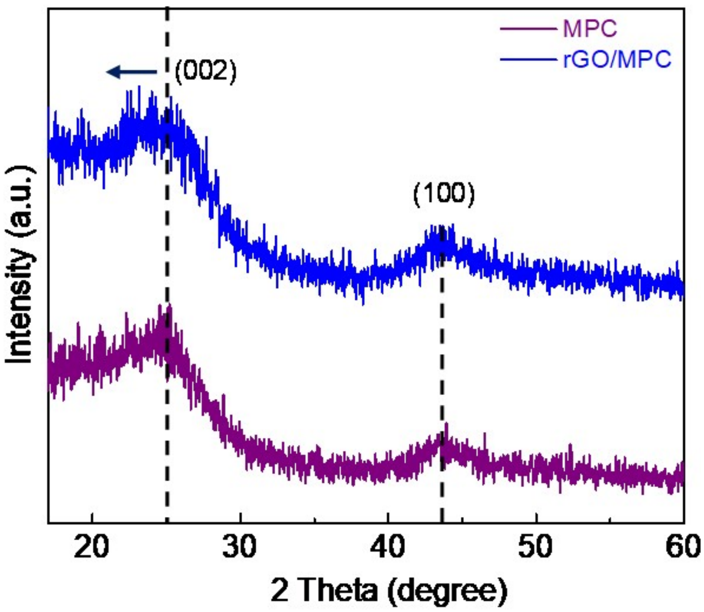

Figure S3. XRD patterns of MPC and rGO/MPC materials.

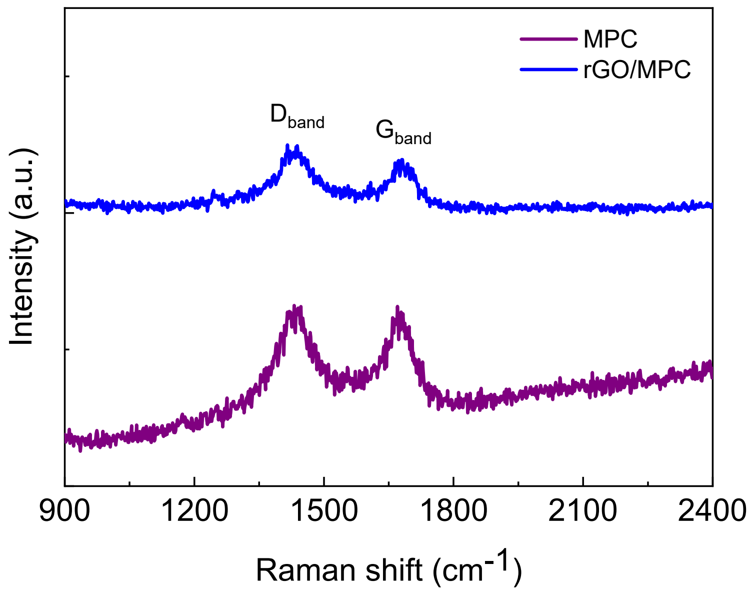

Figure S4. Raman spectra of MPC and rGO/MPC materials.

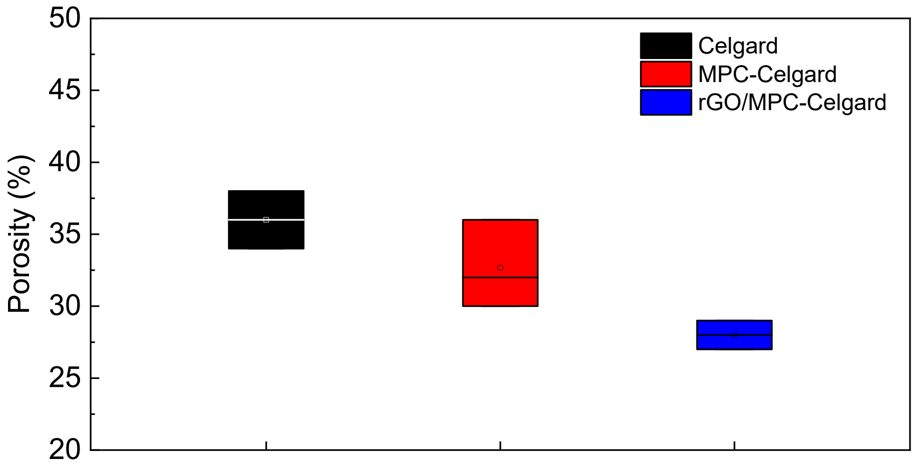

Figure S5. Porosity comparison of uncoated Celgard, MPC-Celgard and rGO/MPC-Celgard separators.

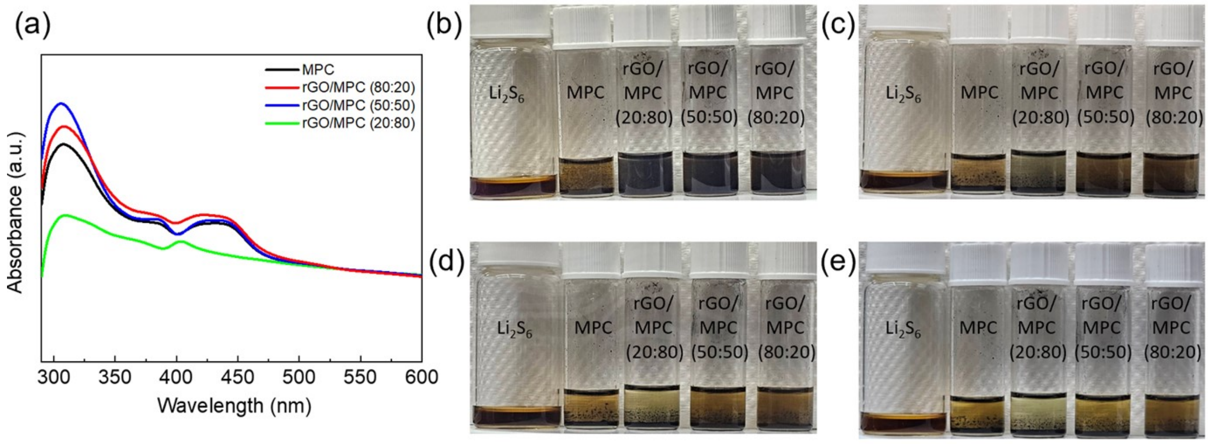

Figure S6. (a) UV-Vis spectra of the Li_2S_6 solution after static adsorption with MPC and rGO/MPC composites for 24 h. Color evolution of the supernatant at (b) 0 h, (c) 1 h, (d) 4 h, and (e) 24 h.

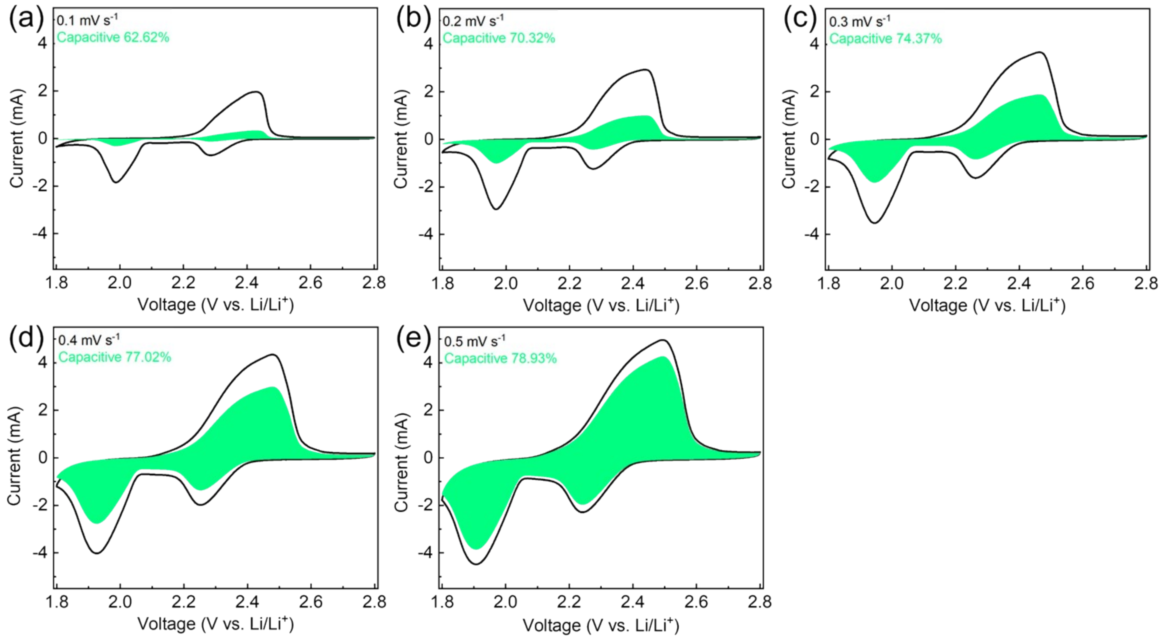

Figure S7. (a-e) CV plots highlighting capacitive-controlled contributions for the rGO/MPC-Celgard separator at various scan rates.

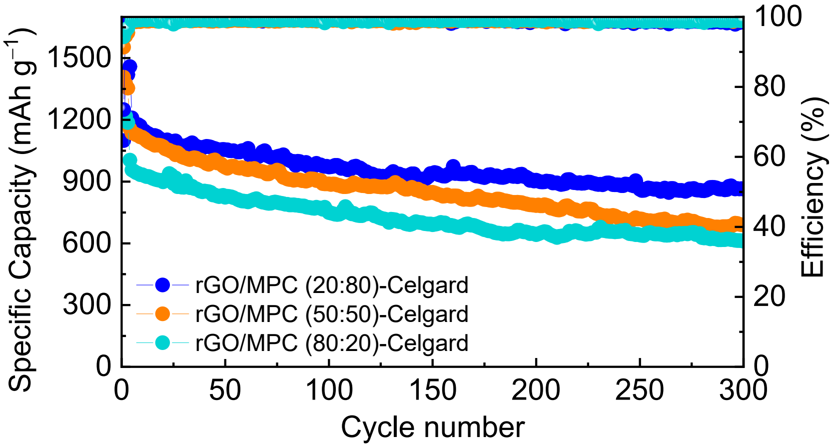

Figure S8. Cycle life data of LSBs with rGO/MPC-Celgard separators at different rGO-to-MPC ratios.

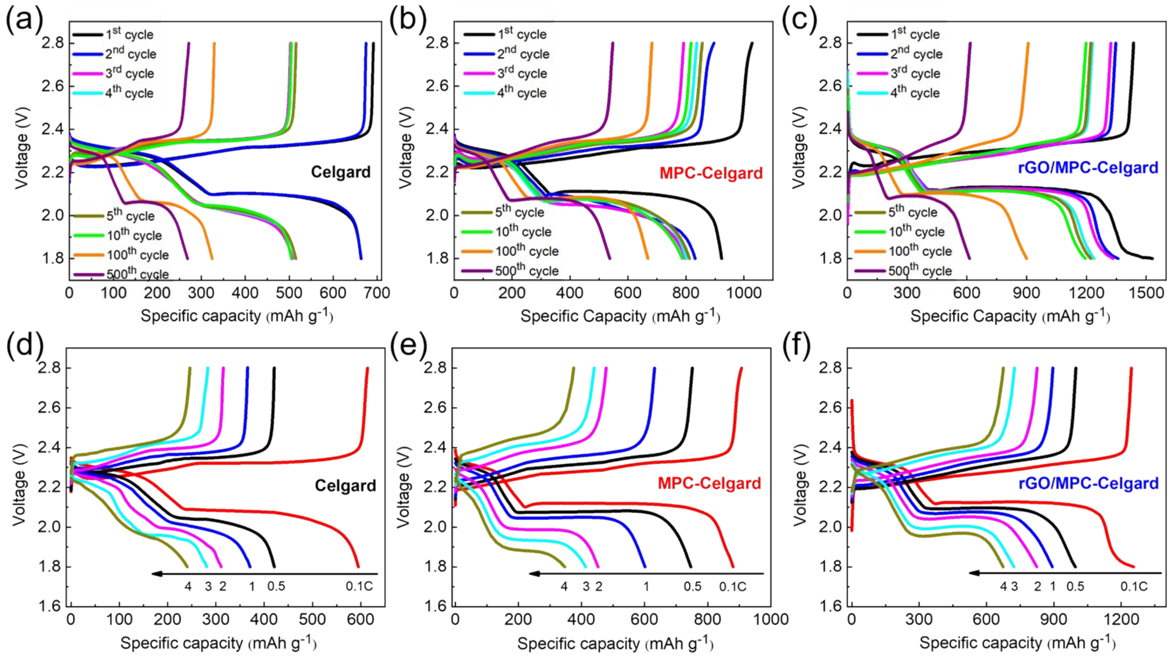

Figure S9. Charge/discharge profiles of LSBs using (a) uncoated Celgard, (b) MPC-Celgard, and (c) rGO/MPC-Celgard separators at different cycle numbers, and (d-f) their profiles at varying C-rates.

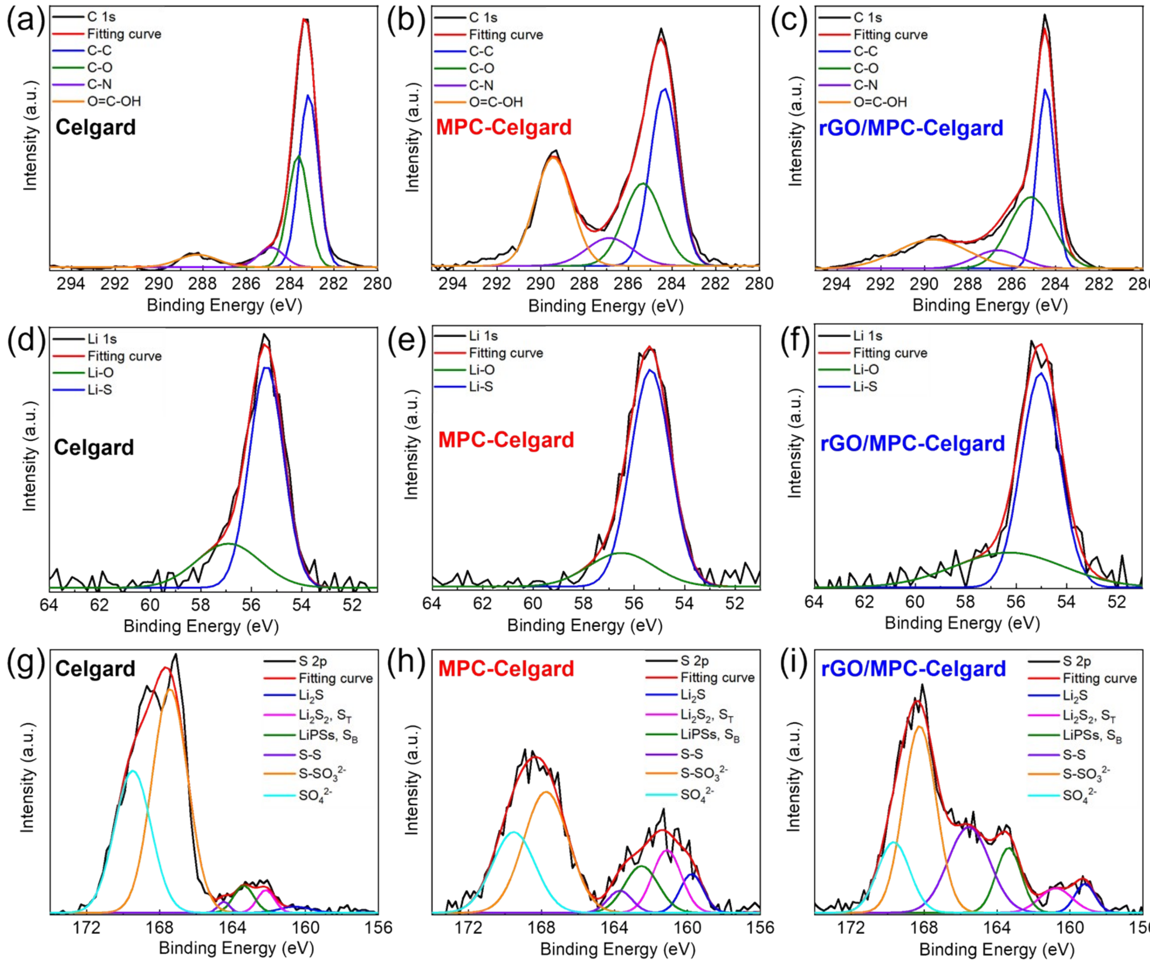

Figure S10. XPS spectra of (a-c) C 1s, (d-f) Li 1s, and (g-i) S 2p for uncoated Celgard, MPC-Celgard, and rGO/MPC-Celgard separators after cycling.

Table S1. Average particle sizes of MPC, heated MPC, GO/MPC, and rGO/MPC materials.

Sample	Particle Size
MPC	224 ± 61 nm
Heated MPC	202 ± 37 nm
GO/MPC	11.9 ± 2.8 μm
rGO/MPC	23.9 ± 7.4 μm

Table S2. Calculated crystallite sizes of MPC and rGO/MPC based on the primary diffraction peaks observed in the XRD patterns.

Sample	Peak Position (2θ)	Plane	FWHM (°)	D (nm)
MPC	24.5°	(002)	5.73	1.42
rGO/MPC	24.1°	(002)	5.7	1.43

The crystallite sizes were calculated using the Scherrer equation:

$$D = K\lambda / \beta\cos\theta$$

where D is the crystallite size, K is the shape factor (0.9), λ is the X-ray wavelength (0.15418 nm for Cu Kα), β is the full width at half maximum (FWHM) in radians, and θ is the Bragg angle.

Table S3. Summary of Li-ion diffusion coefficients (D_{Li^+}; unit: $cm^2\ s^{-1}$) for LSBs assembled with MPC-Celgard and rGO/MPC-Celgard separators.

Sample	Peak A	Peak B	Peak C
MPC-Celgard	5.96E−05	2.7E−06	2.5E−06
rGO/MPC-Celgard	1.72E−04	1.67E−05	9.5E−06

Table S4. Fitted resistance values of LSBs with different separators.

Testing Condition	Resistance	Separator		
		Celgard	MPC-Celgard	rGO/MPC-Celgard
Before cycle	R_e (Ω)	4.5	5.0	2.5
	R_{ct} (Ω)	38.7	42.1	9.4
After 10th charge cycle	R_e (Ω)	6.1	5.3	7.1
	R_i (Ω)	28.9	32.9	12.2
	R_{ct} (Ω)	9.6	9.3	3.3
After 100th charge cycle	R_e (Ω)	12.4	13.0	10.6
	R_i (Ω)	19.0	40.1	8.4
	R_{ct} (Ω)	11.1	4.0	0.5

Table S5. Electrical conductivity of MPC-Celgard and rGO/MPC-Celgard separators with rGO-to-MPC ratios of 20:80, 50:50, and 80:20.

rGO-to-MPC Ratio	Electrical Conductivity (S cm^{-1})
0:100 (MPC)	0.30
20:80	0.97
50:50	0.61
80:20	0.12

Table S6. XPS peak area percentages of sulfur species under various etching durations for LSBs with different separators after cycling.

Separator	Sulfur Species	Peak Area Percentage (%)					
		Surface	30 s	1 min	1.5 min	2 min	2.5 min
Celgard	Li_2S	1.3	9.4	8.2	15.5	13.8	22.5
	Li_2S_2, S_T	2.7	26.6	33.0	31.5	34.2	36.1
	LiPSs, S_B	3.8	12.2	16.9	9.4	11.3	16.7
	S-S	0.9	6.4	2.5	1.9	4.1	3.4
	$S\text{-}SO_3^{2-}$	55.4	25.1	28.0	24.2	21.0	17.3
	SO_4^{2-}	35.9	20.3	11.4	17.5	15.5	4.1
MPC-Celgard	Li_2S	6.5	12.8	22.3	11.3	18.0	19.5
	Li_2S_2, S_T	13.2	28.4	30.2	47.9	39.5	40.1
	LiPSs, S_B	11.5	4.8	7.1	4.2	6.4	8.0
	S-S	3.9	1.6	1.0	2.6	6.2	2.4
	$S\text{-}SO_3^{2-}$	39.7	31.4	23.7	19.0	15.4	14.9
	SO_4^{2-}	25.2	21.0	15.6	15.0	14.5	15.1
rGO/MPC-Celgard	Li_2S	3.9	5.8	6.8	5.5	5.9	2.2
	Li_2S_2, S_T	5.3	10.2	8.5	10.2	8.1	11.5
	LiPSs, S_B	10.9	16.3	19.1	25.1	25.3	25.1
	S-S	23.9	26.3	24.5	22.0	27.8	27.3
	$S\text{-}SO_3^{2-}$	41.0	33.6	32.0	28.4	25.5	29.4
	SO_4^{2-}	15.1	7.7	9.2	8.9	7.4	4.6

Table S7. Comparison of electrochemical performance of modified separators for LSBs from previous studies (1C = 1675 mA g^{-1}).

Separator design	S loading (mg cm^{-2})	(C rate) Cycle #	(C rate) Capacity (mAh g^{-1})	Capacity Retention	Rate Capability	Ref.
rGO/MPC	4.8	(0.5C) 300	(0.1C) 1532	(0.5C) 60.4%	4C	**This work**
KB/US-Mo_2C@PP	4.9	(0.2C) 100	(0.2C) 1212	(0.2C) 86.9%	2C	1
Co_3O_4@GC/N-CNT NF	2.0	(0.1C) 250	(0.1C) 1187	(0.1C) 59.0%	2C	2
VO_2/CNFs-PP	2.0	(0.1C) 200	(0.1C) 1303.8	(0.1C) 52.4%	1C	3
Fe_3S_4/rGO-PP	1.0	(0.2C) 100	(0.2C) 1293	(0.2C) 58.0%	2C	4
$CoSe_2$@CNF	4.1	(0.5C) 275	(0.5C) 1445.6	(0.5C) 58.8%	2C	5
DNA-CNT/MXene/PP	1.0	(0.5C) 100	(0.5C) 920	(0.5C) 76.5%	2C	6
PVIM/PAN	5.0	(0.1C) 100	(0.1C) 1480	(0.1C) 65.4%	2C	7
NiCo@C/CNTs	3.6	(0.5C) 300	(0.5C) 1038.5	(0.5C) 57.8%	3C	8
CoO-CoP-CNT	1.1	(0.5C) 200	(0.5C) 1223.4	(0.5C) 57.3 %	2C	9
Ni_3Sn_2/NG	3.6	(0.2C) 50	(0.2C) 1240	(0.2C) 84.9%	2C	10
N-rGO	1.5	(0.1C) 200	(0.1C) 1308	(0.1C) 83.7%	1C	11

Table S8. Comparison of electrochemical performance of graphene-based composites for LSBs from previous studies (1C = 1675 mA g^{-1}).

Composite design	S loading ($mg\ cm^{-2}$)	(C rate) Cycle #	(C rate) Capacity ($mAh\ g^{-1}$)	Capacity Retention	Rate Capability	Ref.
rGO/MPC	4.8	(0.5C) 300	(0.1C) 1532	(0.5C) 60.4%	4C	**This work**
rGO/activated C	~4	(0.1C) 50	(0.1C) 1100	(0.1C) 99.7%	0.5C	[12]
rGO/porous C	N/A	(0.6C) 500	(0.06C) 1165	(0.6C) ~39%	0.6C	[13]
rGO/N-rich porous C	3	(0.5C) 400	(0.1C) 979.9	(0.5C) 68.1%	2C	[14]
B-N-doped Gn	1.4-1.6	(2C) 700	(0.2C) 1359.9	(2C) 45.4%	3C	[15]
BN/MoS_2/Gn	1-1.2	(5C) 500	(5C) 1268	(5C) 38.6%	5C	[16]
Gn/C/Co_9S_8/porous C	1.2-1.3	(1C) 500	(0.2C) 1256	(1C) 61.1%	3C	[17]

References

1 N. Jiang, G. Jiang, D. Niu, J. Mao, M. Chen, K. Li and Y. Li, *Journal of Energy Chemistry*, 2020, **51**, 207–215.
2 R. Saroha, J. H. Oh, J. S. Lee, Y. C. Kang, S. M. Jeong, D.-W. Kang, C. Cho and J. S. Cho, *Chemical Engineering Journal*, 2021, **426**, 130805.
3 B. Chen, T. Ai, W. Li, H. Dong, J. Wei, J. Li, L. Zhang and Q. Huang, *Journal of Power Sources*, 2024, **613**, 234822.
4 L. Li, H. Liu, B. Jin, Q. Sheng, Q. Li, M. Cui, Y. Li, X. Lang and Q. Jiang, *ACS Applied Nano Materials*, 2023, **6**, 1161–1170.
5 Y. Zhang, Y. Li, C. Xu, D. Li, J. Cao and P. Huo, *Journal of Energy Storage*, 2024, **101**, 113889.
6 Y. Li, M. Li, Y.-C. Zhu, S. Song, S.-N. Li, J. Aarons, L.-C. Tang and J. Bae, *Composites Part B: Engineering*, 2023, **251**, 110465.
7 C. Lin, P. Feng, D. Wang, X. Chen, Y. Fang, Y. Gao, Y. Zheng, Y. Yan and M. Liu, *Advaned Function Materials*, 2024, 2411872.
8 J. Xiong, X. Liu, P. Xia, X. Guo, S. Lu, H. Lei, Y. Zhang and H. Fan, *Journal of Colloid and Interface Science*, 2023, **652**, 1417–1426.
9 H. Jia, S. Li, S. Gao, M. Han, Y. E. and Y. Liu, *Journal of Energy Storage*, 2024, **86**, 111245.
10 X. Qi, L. Huang, Y. Luo, Q. Chen and Y. Chen, *Journal of Colloid and Interface Science*, 2022, **628**, 896–910.
11 A. Srikhaow, J. P. Mensing, J. Lohitkarn, C. Sriprachuabwong, C. Poochai, Y. Choominjak, A. Wisitsoraat, T. Lomas and A. Tuantranont, *Energy Fuels*, 2022, **36**, 13902–13910.
12 G. Jiménez-Martín, J. Castillo, X. Judez, J. L. Gómez-Urbano, G. Moreno-Fernández, A. Santiago, A. Saenz De Buruaga, I. Garbayo, J. A. Coca-Clemente, A. Villaverde, M. Armand, C. Li and D. Carriazo, *Batteries & Supercaps*, 2022, **5**, e202200167.
13 N. Wang, J. Wang, J. Zhao, J. Wang, J. Pan and J. Huang, *Journal of Alloys and Compounds*, 2021, **851**, 156832.
14 J. Xi, J. Liu, Z. Gong, S. Wang, X. Li, J. Yuan, X. Mei and Z. Luo, *Materials Letters*, 2022, **316**, 132050.
15 H. Ci, M. Wang, Z. Sun, C. Wei, J. Cai, C. Lu, G. Cui, Z. Liu and J. Sun, *Journal of Energy Chemistry*, 2022, **66**, 474–482.
16 C. S. Bongu, T. Shafaut and E. H. Alsharaeh, *Energy Fuels*, 2025, **39**, 15876–15887.
17 Q. Wang, J. Cheng, Y. Li, J. Shi, N. Han, X. Zhang, Y. Song, H. Liu and C. Ma, *Journal of Energy Storage*, 2025, **137**, 118489.